A general solution to non-linear particle acceleration at non-relativistic shock waves

E. Amato[★] and P. Blasi[★]

INAF–Osservatorio Astrofisico di Arcetri, Largo E. Fermi, 5, 50125, Firenze, Italy

ABSTRACT

Diffusive acceleration at collisionless shock waves remains one of the most promising acceleration mechanisms for the description of the origin of cosmic rays at all energies. A crucial ingredient to be taken into account is the reaction of accelerated particles on the shock, which in turn determines the efficiency of the process. Here we propose a semi-analytical kinetic method that allows us to calculate the shock modification induced by accelerated particles together with the efficiency for particle acceleration and the spectra of accelerated particles. The shock modification is calculated for arbitrary environment parameters (Mach number, maximum momentum, density) and for arbitrary diffusion properties of the medium. Several dependences of the diffusion coefficient on particle momentum and location are considered to assess the accuracy of the method.

Key words: acceleration of particles – shock waves – cosmic rays.

1 INTRODUCTION

Most scenarios for the origin of cosmic rays rely upon the acceleration of charged particles in the presence of shock waves, developed in sources such as supernova remnants, active galaxies, planetary shocks, gamma-ray bursts and many others. The basic features of the acceleration process have been highlighted in the pioneering papers by Krymskii (1977), Blandford & Ostriker (1978) and Bell (1978) in the context of the so-called 'test particle' assumption. Several excellent reviews (Drury 1983; Blandford & Eichler 1987; Jones & Ellison 1991; Malkov & Drury 2001) discuss in detail the many problems that are still open concerning the acceleration process. Among these, a fundamental one is the limited applicability of the results found within the test particle approach. In most scenarios for the origin of either Galactic or extragalactic cosmic rays, in fact, an appreciable fraction of the kinetic energy crossing the shock needs to be transferred to accelerated particles. This need contradicts the very assumption that the accelerated particles are test particles, unable to exert any dynamical reaction on the shocked fluid. The well-known result that the spectrum of the accelerated particles is a power law with slope nearly independent of the detailed properties of the system (e.g. diffusion coefficient) holds only within the context of this test particle approximation. Relaxing this assumption leads to the modification of the shock by the accelerated particles, a phenomenon that has received much attention in the context of the so-called two-fluid models (Drury & Völk 1980, 1981), kinetic models (Malkov 1997; Malkov, Diamond & Völk 2000; Blasi 2002, 2004) and numerical approaches, both Monte Carlo and other simu-

lation procedures (Bell 1987; Ellison, Möbius & Paschmann 1990; Jones & Ellison 1991; Ellison, Baring & Jones 1995, 1996; Kang & Jones 1997, 2005; Kang, Jones & Gieseler 2002). For an accurate recent review, see the work by Malkov & Drury (2001), from which the reader can see the weak and strong points of each approach. The present paper illustrates a kinetic analytical approach, which provides the exact solution for the spectrum of accelerated particles and shock modification in a very general situation in which the diffusion properties of the medium are arbitrary. The problem is reduced to solving an integral–differential equation, which easily leads to the required solution. For the injection of particles at the shock surface, we implement the recipe previously presented by Blasi, Gabici & Vannoni (2005). In all the cases that we have considered, we have never found evidence for multiple solutions. The method that we propose is of general validity, in that it can be used for an arbitrary momentum dependence of the diffusion coefficient and for diffusion properties (related to the magnetization properties of the medium) that can change in an arbitrary way with the spatial location in the fluid.

2 CALCULATIONS

The equations for the conservation of the mass and momentum fluxes between upstream infinity and a point x in the upstream region can be written as

$$\rho_0 u_0 = \rho(x)u(x), \tag{1}$$

$$\rho_0 u_0^2 + P_{g,0} = \rho(x)u(x)^2 + P_g(x) + P_{CR}(x), \tag{2}$$

where ρ, u and P_g are the gas density, velocity and pressure (the corresponding quantities at upstream infinity are indicated with the

★E-mail: amato@arcetri.astro.it (EA); blasi@arcetri.astro.it (PB)

index 0). The pressure of accelerated particles is defined as

$$P_{\text{CR}}(x) = \frac{1}{3} \int_{p_{\text{inj}}}^{p_{\text{max}}} \text{d}p \, 4\pi p^3 v(p) f(x, p), \tag{3}$$

and $f(x, p)$ is the distribution function of accelerated particles. Here p_{inj} and p_{max} are the injection and maximum momenta. The function f vanishes at upstream infinity, which implies that there are no cosmic rays infinitely distant from the shock in the upstream region. The distribution function satisfies the following transport equation in the reference frame of the shock:

$$\frac{\partial}{\partial x} \left[D(x, p) \frac{\partial}{\partial x} f(x, p) \right] - u \frac{\partial f(x, p)}{\partial x}$$
$$+ \frac{1}{3} \left(\frac{\text{d}u}{\text{d}x} \right) p \frac{\partial f(x, p)}{\partial p} + Q(x, p) = 0. \tag{4}$$

The x-axis is oriented from upstream infinity ($x = -\infty$) to downstream infinity ($x = +\infty$), with the shock located at $x = 0$. The injection is introduced here through the function $Q(x, p)$. The diffusion properties are described by the arbitrary function $D(x, p)$, depending on both momentum and space. In previous approaches, restrictive assumptions on the diffusion coefficient were always adopted in order to facilitate the path to the solution. The solution f can be written in the following implicit form:

$$f(x, p) = \exp\left[-\int_x^0 \text{d}x' \frac{u(x')}{D(x', p)} \right]$$
$$\times \left\{ f_0(p) + \frac{1}{3} \int_x^0 \frac{\text{d}x'}{D(x', p)} \exp\left[\int_{x'}^0 \text{d}x'' \frac{u(x'')}{D(x'', p)} \right] \right.$$
$$\left. \times \frac{1}{p^2} \frac{\partial}{\partial p} \int_{-\infty}^{x'} \text{d}x'' \frac{\text{d}u}{\text{d}x''} [f(x'', p)p^3] \right\}. \tag{5}$$

In the case of a spatially constant diffusion coefficient, as shown by Malkov (1997), a very good approximation to the solution is found in the form

$$f(x, p) = f_0(p) \exp\left[-\frac{q(p)}{3D(p)} \int_x^0 \text{d}x' u(x') \right],$$

with $q(p) = -\text{d} \ln f_0 / \text{d} \ln p$ and $f_0(p) = f(x = 0, p)$ the distribution function at the shock. We have found that the similar form

$$f(x, p) = f_0(p) \exp\left[-\frac{q(p)}{3} \int_x^0 \text{d}x' \frac{u(x')}{D(x', p)} \right] \tag{6}$$

represents a very good approximation for the case of diffusion coefficients with arbitrary spatial dependence (see Section 3). We therefore adopt this functional form in our calculations, although it is not strictly required, in the sense that we could well use the complete solution, equation (5).

It was shown by Blasi (2002) that the function $f_0(p)$ can be written in general as

$$f_0(p) = \left[\frac{3R_{\text{tot}}}{R_{\text{tot}}U(p) - 1} \right] \frac{\eta n_0}{4\pi p_{\text{inj}}^3} \exp\left[-\int_{p_{\text{inj}}}^p \frac{\text{d}p'}{p'} \frac{3R_{\text{tot}}U(p')}{R_{\text{tot}}U(p') - 1} \right]. \tag{7}$$

Here we have introduced the function $U(p) = u_p/u_0$, with

$$u_p = u_1 - \frac{1}{f_0(p)} \int_{-\infty}^0 \text{d}x (\text{d}u/\text{d}x) f(x, p) \tag{8}$$

where u_1 is the fluid velocity immediately upstream (at $x = 0^-$). We have used

$$Q(x, p) = \frac{\eta n_{\text{gas},1} u_1}{4\pi p_{\text{inj}}^2} \delta(p - p_{\text{inj}}) \delta(x),$$

with $n_{\text{gas},1} = n_0 R_{\text{tot}} / R_{\text{sub}}$ the gas density immediately upstream ($x = 0^-$) and η the fraction of the particles crossing the shock that are going to take part in the acceleration process. In equation (7) we have also introduced the two quantities $R_{\text{sub}} = u_1/u_2$ (compression factor at the subshock) and $R_{\text{tot}} = u_0/u_2$ (total compression factor). The two compression factors, assuming for simplicity that the heating is only adiabatic, are related through the following expression (Blasi 2002):

$$R_{\text{tot}} = M_0^{2/(\gamma_{\text{g}}+1)} \left[\frac{(\gamma_{\text{g}} + 1)R_{\text{sub}}^{\gamma_{\text{g}}} - (\gamma_{\text{g}} - 1)R_{\text{sub}}^{\gamma_{\text{g}}+1}}{2} \right]^{1/(\gamma_{\text{g}}+1)}, \tag{9}$$

where M_0 is the Mach number of the fluid at upstream infinity and γ_{g} is the ratio of specific heats for the fluid. The parameter η in equation (7) contains the very important information about the injection of particles from the thermal bath. Following the work of Blasi et al. (2005), we relate η to the compression factor at the subshock as

$$\eta = \frac{4}{3\pi^{1/2}} (R_{\text{sub}} - 1) \xi^3 e^{-\xi^2}. \tag{10}$$

Here ξ is a parameter that identifies the injection momentum as a multiple of the momentum of the thermal particles in the downstream section ($p_{\text{inj}} = \xi p_{\text{th},2}$). This recipe is inspired by the 'thermal leakage model' originally presented by Gieseler, Jones & Kang (2000) [see also previous work by Ellison, Jones & Eichler (1981), Ellison (1981) and Ellison & Eichler (1984)]. The parameter ξ is supposed to contain the information about the microscopic structure of the shock. For collisionless shock waves the thickness of the shock is expected to be of the order of the Larmor radius of the thermal particles in the shock vicinity, which is not a very well-defined concept because of the violent fluctuations in the electromagnetic fields within the shock. A simple argument can be used to infer that ξ is of the order of 2–4 (Blasi et al. 2005). For the numerical calculations that follow, we always use $\xi = 3.5$, which allows for only a fraction of the order of 10^{-4} of the particles crossing the shock to be injected in the accelerator.

Equation (2) for the conservation of the momentum flux, once normalized to $\rho_0 u_0^2$, is easily transformed to

$$\xi_{\text{c}}(x) = 1 + \frac{1}{\gamma_{\text{g}} M_0^2} - U(x) - \frac{1}{\gamma_{\text{g}} M_0^2} U(x)^{-\gamma_{\text{g}}}, \tag{11}$$

where $\xi_{\text{c}}(x) = P_{\text{CR}}(x)/\rho_0 u_0^2$ and $U(x) = u(x)/u_0$. In terms of the distribution function (equation 6), we can also write

$$\xi_{\text{c}}(x) = \frac{4\pi}{3\rho_0 u_0^2} \int_{p_{\text{inj}}}^{p_{\text{max}}} \text{d}p \, p^3 v(p) f_0(p) \exp\left[-\int_x^0 \text{d}x' \frac{U(x')}{x_p(x', p)} \right], \tag{12}$$

where for simplicity we have introduced $x_p(x, p) = 3D(p, x)/q(p)u_0$.

By differentiating equation (12) with respect to x we obtain

$$\frac{\text{d}\xi_{\text{c}}}{\text{d}x} = \lambda(x)\xi_{\text{c}}(x)U(x), \tag{13}$$

where
$$\lambda(x) = \langle 1/x_p \rangle_{\xi_{\text{c}}}$$

$$= \frac{\int_{p_{\text{inj}}}^{p_{\text{max}}} \text{d}p \, p^3 \frac{1}{x_p(x,p)} v(p) f_0(p) \exp\left[-\int_x^0 \text{d}x' \frac{U(x')}{x_p(x',p)} \right]}{\int_{p_{\text{inj}}}^{p_{\text{max}}} \text{d}p \, p^3 v(p) f_0(p) \exp\left[-\int_x^0 \text{d}x' \frac{U(x')}{x_p(x',p)} \right]}, \tag{14}$$

and $U(x)$ is expressed as a function of $\xi_{\text{c}}(x)$ through equation (11).

Finally, after integration by parts of equation (8), one is able to express $U(p)$ in terms of an integration involving $U(x)$ alone:

$$U(p) = \int_{-\infty}^{0} dx \, U(x)^2 \frac{1}{x_p(x, p)} \exp\left[-\int_{x}^{0} dx' \frac{U(x')}{x_p(x', p)}\right] \quad (15)$$

which allows $f_0(p)$ to be easily calculated through equation (7).

Equations (11) and (13) can be solved by iteration in the following way: for a fixed value of the compression factor at the subshock, R_{sub}, the value of the dimensionless velocity at the shock is calculated as $U(0) = R_{sub}/R_{tot}$. The corresponding pressure in the form of accelerated particles is given by equation (11) as

$$\xi_c(0) = 1 + \frac{1}{\gamma_g M_0^2} - \frac{R_{sub}}{R_{tot}} - \frac{1}{\gamma_g M_0^2} \left(\frac{R_{sub}}{R_{tot}}\right)^{-\gamma_g}.$$

This is used as a boundary condition for equation (13), where the functions $U(x)$ and $\lambda(x)$ [and therefore $f_0(p)$] on the right-hand side at the kth step of iteration are taken as the functions at the step $(k-1)$. In this way the solution of equation (11) at the step k is simply

$$\xi_c^{(k)}(x) = \xi_c(0) \exp\left[-\int_{x}^{0} dx' \lambda^{(k-1)}(x') U^{(k-1)}(x')\right], \quad (16)$$

with the correct limits when $x \to 0$ and $x \to -\infty$. At each step of iteration the functions $U(x)$, $f_0(p)$ and $\lambda(x)$ are recalculated [through equations (11), (15), (7) and (14)], until convergence is reached. The solution of this set of equations, however, is also a solution of our physical problem only if the pressure in the form of accelerated particles as given by equation (11) coincides with that calculated by using the final $f_0(p)$ in equation (12). This occurs only for one specific value of R_{sub}, which fully determines the solution of our problem.

3 RESULTS

The computational method illustrated in the previous section is very fast and allows one to determine the solution (namely the velocity and density profiles in the precursor, the density of accelerated particles as a function of momentum and location in the upstream fluid, and all the thermodynamic quantities related to the gas) for an arbitrary choice of the diffusion coefficient and for any values of the environmental parameters (Mach number, density, maximum momentum).

In Fig. 1 we illustrate the spectra (upper panel) and slopes (lower panel) as a function of momentum for the following values of the Mach number: $M_0 = 4$ (dotted line), 10 (short-dashed line), 50 (dash–dotted line), 100 (triple-dot–dashed line), 300 (long-dashed line) and 500 (solid line). The distribution functions are multiplied by p^4 to emphasize the concave shape of the modified spectra. All the curves refer to $p_{max} = 10^5$ in units of mc. The most evident aspect of shock modification, found in all previous calculations, is here confirmed: the shock modification is enhanced when the Mach number of the shock increases. The spectrum is flatter at high momenta as confirmed by the lower panel of Fig. 1, and easily understood in terms of the large values of the total compression factor (see Table 1).

For strongly modified shocks, the slope becomes even flatter than $p^{-3.5}$ at high momenta, as also found in numerical simulations (Berezhko & Ellison 1999, and references therein).[1] In these

---

[1] We remind the reader that in other semi-analytical calculations (e.g. Malkov 1997) the asymptotic spectrum for $p_{inj} \ll p < p_{max}$ has slope 3.5.
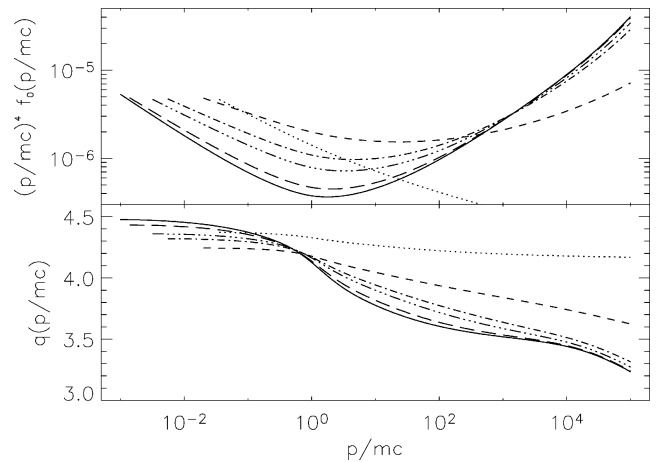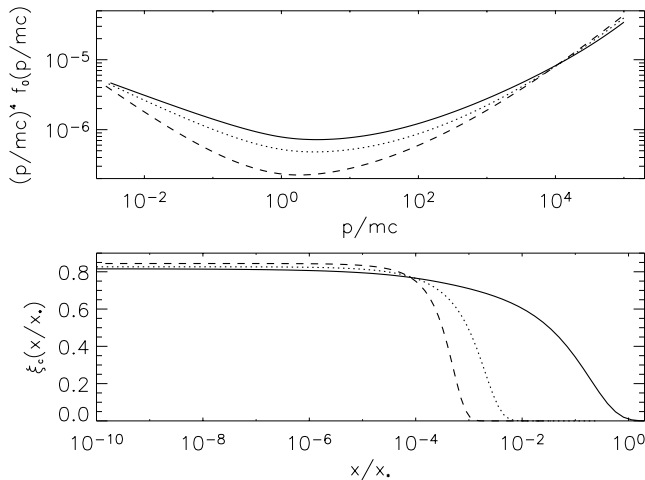

Figure 1. Upper panel: spectra of accelerated particles at the location of the shock for $M_0 = 4$ (dotted line), 10 (short-dashed line), 50 (dash–dotted line), 100 (triple-dot–dashed line), 300 (long-dashed line) and 500 (solid line). Lower panel: momentum-dependent slope for the same values of Mach numbers. In both panels we used $\xi = 3.5$ and $p_{max} = 10^5 mc$.

Table 1. Shock modification for different Mach numbers.

Mach number M_0	R_{sub}	R_{tot}	$\xi_c(0)$	p_{inj}	η
4	3.19	3.57	0.1	0.035	3.4×10^{-4}
10	3.413	6.57	0.47	0.02	3.7×10^{-4}
50	3.27	23.18	0.85	0.005	3.5×10^{-4}
100	3.21	39.76	0.91	0.0032	3.4×10^{-4}
300	3.19	91.06	0.96	0.0014	3.4×10^{-4}
500	3.29	129.57	0.97	0.001	3.5×10^{-4}

conditions, most energy is channelled in the highest energy part of the spectrum. At lower energies, on the other hand, the spectrum is steeper than that predicted by linear theory, as a natural consequence of the lower compression at the subshock for strongly modified shocks. For the parameters adopted here, the energy saturation [namely $\xi_c(0) \sim 1$] is achieved for Mach numbers around 100, as demonstrated by the fact that the corresponding curves in the upper panel of Fig. 1 have roughly the same height (namely the same energy content). On the other hand, different modifications result in different compressions at the subshock and therefore different injection momenta. This is illustrated in Fig. 1 and Table 1. In particular, in Table 1 we list the values of the compression factors, dimensionless cosmic ray pressure at the shock, injection momentum and fraction of accelerated particles for the same values of M_0 used to obtain the curves in Fig. 1.

In Fig. 2 we illustrate the results of our method for different choices of the momentum dependence of the diffusion coefficient. We consider three cases: (1) Bohm diffusion, $D_B(p) \propto p$; (2) Kraichnan diffusion, $D_{Kr}(p) \propto p^{1/2}$; and (3) Kolmogorov diffusion, $D_{Kol}(p) \propto p^{1/3}$ (relativistic scalings). For illustrative purposes, we choose to calculate the spectrum of accelerated particles and the shock modification for $M_0 = 100$ and $p_{max} = 10^5 mc$. The resulting spectrum is shown in the upper panel of Fig. 2, for Bohm diffusion (solid line), Kraichnan diffusion (dotted line) and Kolmogorov diffusion (dashed line). The general tendency is that the saturation phenomenon occurs at somewhat lower Mach numbers for diffusion coefficients that depend more weakly on momentum. The lower panel in Fig. 2 illustrates the spatial distribution of pressure in the accelerated particles [$\xi_c(x)$], where the spatial coordinate is chosen

Figure 2. Upper panel: spectra of accelerated particles at the location of the shock for $M_0 = 100$, $p_{max} = 10^5 mc$ and for a Bohm diffusion coefficient (solid line), Kraichnan diffusion coefficient (dotted line) and Kolmogorov diffusion coefficient (dashed line). Lower panel: distribution of the pressure in the form of accelerated particles, normalized to the ram pressure [$\xi_c(x)$ as defined by equations (11)–(12)], for the same three cases. The spatial coordinate is in units of $x_* = D_B(p_{max})/u_0$, with D_B the Bohm diffusion coefficient.

in such a way that $x = 1$ in the point $x_* = D_B(p_{max})/u_0$. Clearly the particles with the maximum momentum diffuse on shorter spatial scales than x_* for diffusion coefficients with weaker momentum dependence.

The power of the computational method in being suitable for treating arbitrary dependences of the diffusion coefficient on momentum and spatial coordinates is further demonstrated in Fig. 3,
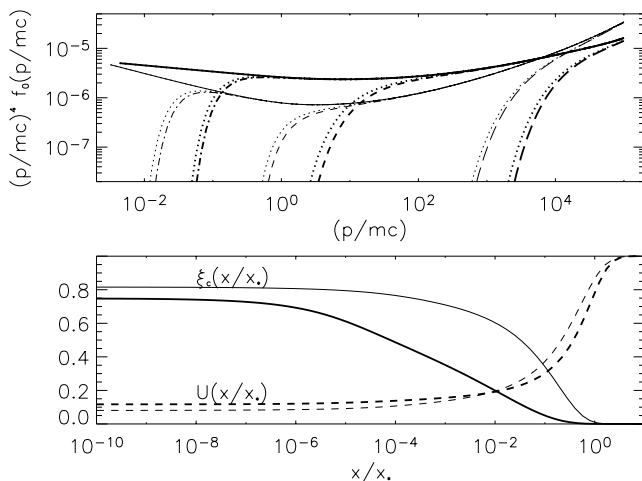
Figure 3. Upper panel: spectra of the accelerated particles for spatially constant Bohm diffusion (thin lines) and for Bohm diffusion with $D(p, x) \propto p/\rho(x)$. The different line types refer, for each case, to $x = 0$ (solid line), $x = 10^{-7}x_*$ (dot–dashed line), $x = 10^{-4}x_*$ (short-dashed line) and $x = 0.1x_*$ (long-dashed line). The dotted lines neighbouring each curve refer to the distribution functions computed by using in the right-hand side of equation (5) the solution obtained with our method (see text for details). Lower panel: $\xi_c(x)$ and $U(x)$ (solid and dashed lines, respectively) for the case of spatially constant Bohm diffusion (thin lines) and for $D(p, x) \propto p/\rho(x)$ (thick lines). The spatial coordinate is again in units of x_* defined as for Fig. 2.

where we show how the solutions change when the diffusion coefficient is allowed to vary in space. For illustrative purposes we consider the case of a Bohm diffusion coefficient with $D_B(p, x) \propto p$ (constant in space) and $D_B(p, x) \propto p/\rho(x)$, where $\rho(x)$ is the gas density at the position x, self-consistently calculated by using the conservation laws. The latter dependence is representative of the case of a magnetic field frozen in the plasma flowing in the upstream section.

In the upper panel of Fig. 3 we plot the spectra of the accelerated particles for spatially constant Bohm diffusion (thin curves) and for $D_B(p, x) \propto p/\rho(x)$ (thick lines). The different line types refer to spectra at the different spatial locations: $x = 0$ (solid line), $x = 10^{-7}x_*$ (dot–dashed line), $x = 10^{-4}x_*$ (short-dashed line) and $x = 0.1x_*$ (long-dashed line), where x_* is defined as above, i.e. $x_* = D_B(p_{max})/u_0$ with D_B referring to the spatially constant Bohm diffusion coefficient. In the lower panel we plot $\xi_c(x)$ (solid lines) and $U(x)$ (dashed lines) for the same two cases, identified by the different thickness of the lines.

In order to assess the goodness of our approximate solution (equation 6), we computed the right-hand side of equation (5) by using the functions $U(x)$ and $f(x, p)$ found with our method. The correction is found to be non-negligible only in the exponentially decreasing parts of the spectrum (see dotted lines in Fig. 3), which contains negligible energy and hardly leads to any observable features. On this basis, we conclude that equation (6) is an excellent approximation to the solution for diffusion coefficients with arbitrary spatial and momentum dependences.

The solutions obtained with this method are remarkably similar to those obtained with approximate methods by Blasi (2002, 2004), for the case of Bohm diffusion with no spatial dependence. The discrepancies with such previous treatments are expected and indeed appear for increasingly weaker dependences of the diffusion coefficient on the momentum of the particles, and in general when a spatial dependence of the diffusion properties is added (these aspects will be discussed in an upcoming detailed paper). The results also compare well with a previous method proposed by Malkov (1997) and Malkov et al. (2000), where the contribution of gas pressure was neglected and no recipe for injection was adopted.

The most important property of the method here described, however, is the fact that it appears to be the first that allows the spatial dependence of the diffusion coefficient to be taken into account. The importance of being able to deal with arbitrary diffusion properties is highlighted by the following considerations. First, particle acceleration at shocks is expected to be efficient only if the turbulence responsible for diffusion is self-generated (Lagage & Cesarsky 1983; Lucek & Bell 2000; Bell 2004), and in this case the diffusion coefficient is necessarily dependent upon both momentum and space in a complex manner. Moreover, the appearance of a maximum momentum is indeed due to the fact that, at some distance from the shock, diffusion becomes ineffective and particles are no longer trapped in the shock vicinity. Since the shock modification depends in a crucial way on the value of the maximum momentum, it is clear that a careful calculation of the shock modification should be able to account for these phenomena.

REFERENCES

Bell A. R., 1978, MNRAS, 182, 443
Bell A. R., 1987, MNRAS, 225, 615
Bell A. R., 2004, MNRAS, 353, 550
Berezhko E. G., Ellison D. C., 1999, ApJ, 526, 385
Blandford R. D., Eichler D., 1987, Phys. Rep., 154, 1
Blandford R. D., Ostriker J. P., 1978, ApJ, 221, L29
Blasi P., 2002, Astropart. Phys. 16, 429
Blasi P., 2004, Astropart. Phys., 21, 45
Blasi P., Gabici S., Vannoni G., 2005, MNRAS, 361, 907
Drury L. O'C., 1983, Rep. Prog. Phys., 46, 973
Drury L. O'C., Völk H. J., 1980, in Setti G., Spada G., Wolfendale A., eds, Proc. IAU Symp. 94, Origin of Cosmic Rays. D. Reidel Publishing, Dordrecht, p. 363
Drury L. O'C., Völk H. J., 1981, ApJ, 248, 344
Ellison D. C., 1981, Geophys. Res. Lett., 8, 991
Ellison D. C., Eichler D., 1984, ApJ, 286, 691
Ellison D. C., Jones F. C., Eichler D., 1981, J. Geophys., 50, 110
Ellison D. C., Möbius E., Paschmann G., 1990, ApJ, 352, 376
Ellison D. C., Baring M. G., Jones F. C., 1995, ApJ, 453, 873
Ellison D. C., Baring M. G., Jones F. C., 1996, ApJ, 473, 1029
Gieseler U. D. J., Jones T. W., Kang H., 2000, A&A, 364, 911
Jones F. C., Ellison D. C., 1991, Space Sci. Rev., 58, 259
Kang H., Jones T. W., 1997, ApJ, 476, 875
Kang H., Jones T. W., 2005, ApJ, 620, 44
Kang H., Jones T. W., Gieseler U. D. J., 2002, ApJ, 579, 337
Krymskii G. F., 1977, Sov. Phys. – Dokl., 327, 328
Lagage P. O., Cesarsky C. J., 1983, A&A, 118, 223
Lucek S. G., Bell A. R., 2000, MNRAS, 314, 65
Malkov M. A., 1997, ApJ, 485, 638
Malkov M. A., Drury L. O'C., 2001, Rep. Prog. Phys., 64, 429
Malkov M. A., Diamond P. H., Völk H. J., 2000, ApJ, 533, L171

This paper has been typeset from a TEX/LATEX file prepared by the author.